Three-Wire Configuration for Resistive Sensor Measurement Using the Analog-to-Digital Converters of Microcontrollers

Apinan Aurasopon
Faculty of Engineering, Mahasarakham University, Mahasakham, Thailand
apinan.a@msu.ac.th

Jirapong Jittakort
Department of Electrical Engineering, Faculty of Technical Education, Rajamangala University of Technology, Thanyaburi, Pathum Thani, Thailand
jirapong_j@rmutt.ac.th (corresponding author)

Received: 5 September 2025 | Revised: 27 September 2025 | Accepted: 12 October 2025

 DOI: https://doi.org/10.48084/etasr.14549

ABSTRACT

This paper presents a simple and effective three-wire configuration for accurate resistive sensor measurement using the Analog-to-Digital Converters (ADCs) of microcontrollers. The proposed method compensates for lead-wire resistance, a major source of error in long-wire sensor installations, without requiring additional analog circuitry or complex signal conditioning. The configuration is based on the Anderson current loop and exploits the internal resistances of microcontroller I/O pins to stabilize the current path. It uses a single ADC with four channels and two digital output pins to control the supply path of the measurement circuit. This architecture simplifies circuit design, reduces component count, and lowers system cost and power consumption. Experimental validation with resistances in the Resistance Temperature Detector (RTD) 1000 range (500–3,500 Ω) confirms high measurement accuracy, achieving a maximum uncertainty of 0.16%. The method is well-suited for practical, low-power, and cost-sensitive resistive sensing applications in embedded and Internet of Things (IoT)-based temperature monitoring systems.

Keywords-three-wire configuration; resistive sensor measurement; Analog-to-Digital Converters (ADCs); microcontrollers; lead wire compensation; RTD1000; Anderson current loop; uncertainty error; Internet of Things (IoT) applications; embedded systems

I. INTRODUCTION

Resistive sensors are commonly used in various industrial and scientific applications for measuring physical quantities such as temperature, displacement, humidity, and pressure. Among them, Resistance Temperature Detectors (RTDs) are widely used due to their high accuracy, long-term stability, and reliable linear response over a broad temperature range [1, 2]. Accurate RTD resistance measurement is essential for applications such as temperature regulation, environmental monitoring, and process automation. These applications often demand high precision and reliability, especially in industrial settings where temperature plays a critical role in maintaining system performance and safety. However, when using a two-wire configuration in remote sensor placements, long lead wires introduce parasitic resistance, which can significantly degrade measurement accuracy. This lead-wire resistance becomes indistinguishable from the sensor resistance, resulting in overestimated temperature readings. Moreover, the resistance of the lead wires is temperature dependent due to the material's temperature coefficient, further complicating precise measurements [3, 4]. As ambient conditions fluctuate, the lead wire resistance may vary dynamically, introducing additional uncertainty and drift in the sensor output. Therefore, compensating for lead resistance is essential in ensuring consistent and accurate RTD-based measurements over time and varying environmental conditions.

Several compensation strategies have been proposed to address lead-wire resistance issues in two-wire RTD systems. These include the use of analog circuits with matched resistors, switching techniques that alternate current paths to isolate wire resistance, and diode-based methods that exploit voltage asymmetry to distinguish between sensor and lead contributions. While these techniques aim to improve accuracy without requiring a full three- or four-wire configuration, they often involve trade-offs in terms of circuit complexity, component count, or calibration requirements. A detailed discussion and classification of such approaches can be found in [5], which reviews a wide range of readout circuits for

remote resistive sensors and highlights their respective advantages and limitations.

To achieve accurate RTD resistance measurement in three-wire and four-wire configurations, Analog Front-End (AFE) circuits typically employ two primary conversion techniques: Resistance-to-Time (R-to-T) and Resistance-to-Voltage (R-to-V). R-to-T conversion determines resistance by measuring timing intervals and translating them into digital signals with a linear transfer function [6-8], whereas R-to-V conversion estimates resistance from voltage measurements across the RTD, which are subsequently processed by a microcontroller [9-11]. A comprehensive overview of such AFE-based techniques, including their application to two-, three-, and four-wire topologies, is provided in [5]. Although effective, these methods generally require additional components such as operational amplifiers (op-amps), controlled switches, constant voltage sources, and passive devices—factors that contribute to increased circuit complexity, power consumption, and cost.

To reduce cost and energy consumption, a Direct Interface Circuit (DIC) based on R-to-T conversion has been proposed, where the sensor is directly connected to the microcontroller without requiring an amplifier. In [12], a three-wire configuration using a DIC achieves high accuracy with a simple design consisting of three resistors and a capacitor, whereas [13] introduces a four-wire configuration that incorporates an additional switch, improving measurement accuracy at the expense of increased circuit complexity. However, these configurations may be susceptible to errors caused by power supply interference, timer jitter, and the internal resistance of microcontroller output pins [14]. The R-to-V method has been developed to simplify resistive sensor measurements while optimizing cost and energy efficiency. Authors in [15] proposed a configuration utilizing the Anderson current loop for two-wire RTD1000 sensors, incorporating a precision reference resistor and two stabilizer resistors to mitigate supply variations and Analog-to-Digital Converter (ADC)-related errors, such as gain (β) and offset (D_{offset}) inaccuracies. Additionally, software-based implementations of R-to-V approaches, such as LabVIEW-based linearization techniques using voltage divider and improved bridge circuits, have been explored to improve accuracy and flexibility [16]. However, this method does not account for lead-wire resistance, which is crucial in remote sensing applications. To overcome this limitation, our previous work [17] introduced three-wire and four-wire configurations based on the Anderson current loop, incorporating external stabilizing resistors along with a tuning method to enhance measurement accuracy.

In contrast, the present work proposes a simplified three-wire configuration that also follows the Anderson current loop principle but replaces the external stabilizing resistors with the internal resistance of microcontroller I/O pins. The configuration uses a single ADC with four channels and two digital output pins to control the supply voltage for the measurement circuit. This design effectively compensates for lead-wire resistance, reduces circuit complexity, and eliminates the need for additional analog components. As a result, the proposed approach achieves lower cost, reduced power consumption, and high measurement accuracy for resistive sensors.

II. THREE WIRE RESISTANCE COMPENSATION

This section presents the configuration for three-wire lead resistance compensation, along with its operating principle and uncertainty analysis.

A. Proposed Configuration for Lead-Wire Compensation

The circuit diagram of the proposed lead-wire compensation platform for three-wire-connected resistive sensors, based on the Anderson current loop configuration, is shown in Figure 1. This approach enables accurate resistance measurement of sensors such as RTDs by effectively compensating for lead-wire resistances (R_{w1}, R_{w2} and R_{w3}) in the three-wire configuration. During measurement cycle, P1 is set as an output and applies a voltage (V_{DD}), whereas P2 is set as ground. This setup establishes a current (I_{ref}) that flows through the reference resistor (R_{ref}), lead-wire resistances (R_{w1} and R_{w3}), the sensor resistance (R_x), and the internal switch resistances (R_p and R_n). Once the measurement is complete, P1 and P2 are set to an input state to reduce energy consumption.

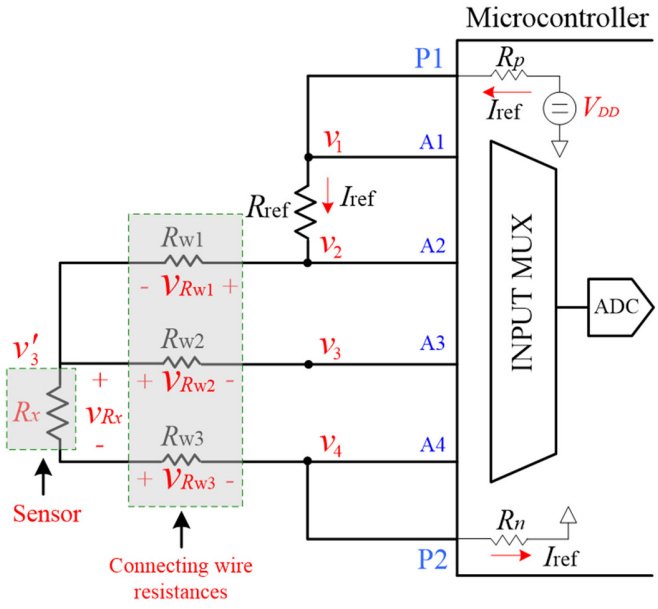

Fig. 1. Proposed three-wire configuration for lead-resistance compensation using ADC measurements. The circuit employs a precision reference resistor and multiple ADC channels to accurately measure the sensor resistance R_x while compensating for the voltage drops across the connecting-wire resistances R_{w1} and R_{w3}.

The circuit utilizes ratiometric voltage measurements at specific nodes, capturing voltage drops (v_1, v_2, v_3, and v_4), which are then sampled by the microcontroller's ADC to calculate R_x while compensating for lead-wire variations. Each ADC channel requires 120 µs for a complete operation, necessitating a minimum measurement cycle of 480 µs to ensure accurate readings, as described on page 285 of [18].

B. Measurement Operating Principle

To measure R_x, the excitation current I_{ref} is assumed to be constant during the measurement cycle. The voltage difference $v_{12} = v_1 - v_2$ represents the potential drop across the reference resistor R_{ref}. Consequently, I_{ref} is given by:

$$I_{\text{ref}} = \frac{v_1 - v_2}{R_{\text{ref}}} \quad (1)$$

Considering the voltage difference between node v_2 and node v_4 ($v_{24} = v_2 - v_4$), the relationship can be expressed as:

$$v_{24} = I_{\text{ref}} \cdot (R_{\text{w1}} + R_x + R_{\text{w3}}) \quad (2)$$

Next, considering the voltage difference between node v_3 and node v_4 ($v_{34} = v_3 - v_4$), and noting that there is no current through R_{w2} (hence $vR_{\text{w2}} = 0$ and $v_3 = v_3'$), we obtain:

$$v_{34} = I_{\text{ref}} \cdot (R_x + R_{\text{w3}}) \quad (3)$$

Combining (2) and (3), and substituting I_{ref}, we can solve for R_x:

$$R_x = R_{\text{ref}} \cdot \left(\frac{2v_{34} - v_{24}}{v_1 - v_2}\right) + R_{\text{w1}} - R_{\text{w3}} \quad (4)$$

Equation (4) indicates that measurement errors can occur if the lead-wire resistances are mismatched ($R_{\text{w1}} \neq R_{\text{w3}}$). However, in practical implementations, the lead wires are typically made from the same material and have the same length, ensuring that $R_{\text{w1}} \approx R_{\text{w3}}$. Under this condition, (4) simplifies to:

$$R_x = R_{\text{ref}} \cdot \frac{2(v_3 - v_4) - (v_2 - v_4)}{(v_1 - v_2)} \quad (5)$$

In addition to compensating for lead-wire resistance errors, this approach inherently rejects the influence of V_{DD} variations and internal resistance changes. Variations in V_{DD} proportionally affect both the numerator and denominator in the ratiometric voltage measurements, resulting in their cancellation. Similarly, changes in internal resistance cause proportional changes in the voltage at each node, but these changes do not affect the final result due to the ratiometric measurement technique. Each voltage v_m represents the voltage measured at node $m = 1, 2, \ldots, 4$, is sequentially digitized by the microcontroller's ADC, where β and D_{offset} errors are introduced. The effect of these errors is represented by the following relationship [15]:

$$v_m = D_m \cdot \frac{V_{\text{ref}}}{N} \cdot \beta + D_{\text{offset}} \cdot \frac{V_{\text{ref}}}{N} \quad (6)$$

where N denotes the ADC resolution in bits, and D_m is the corresponding digital value from the ADC data register. With V_{ref} set to V_{DD}, substituting (6) into (5) yields:

$$R_x = R_{\text{ref}} \cdot \frac{2(D_3 - D_4) - (D_2 - D_4)}{(D_1 - D_2)} \quad (7)$$

When $D_1 > D_2 > D_3 > D_4$, the subtraction and division operations in (7) effectively eliminate β and D_{offset} errors, resulting in an expression for R_x that depends only on the digital values D_m and the known reference resistance R_{ref}. However, residual ADC errors, such as Integral Nonlinearity (INL), Differential Nonlinearity (DNL), and noise, persist and cannot be fully corrected through circuit design or compensation. Although the input current of the ADC Multiplexer (MUX) could be a potential source of error, it is not a significant concern in this configuration. The proposed circuit maintains an output impedance below 10 kΩ, which is within the ADC's specifications [18]. This ensures that the ADC's sampling capacitor charges rapidly, minimizing input lag. However, transient disturbances may occur when switching channels, due to charge redistribution within the ADC's sampling circuit. To mitigate this, a dummy conversion introduces a small delay after selecting the next channel, allowing the capacitor to fully stabilize before taking an actual measurement, thereby reducing potential inaccuracies.

C. Uncertainty Measurement Analysis

The Anderson current loop configuration effectively cancels supply deviations, as well as β and D_{offset} errors. However, additional uncertainty arises from ADC errors, denoted as ΔD, which represent the combined effects of INL and DNL, measured in Least Significant Bits (LSB). These ADC errors directly affect the accuracy of R_x measurements, with the impact of ΔD on the measurement uncertainty calculated as follows [17]:

$$\left|\frac{\Delta R_{D1}}{R_x}\right| = \left|\frac{\partial R_x}{\partial D_1} \cdot \frac{\Delta D}{R_x}\right| = \frac{1}{D_1 - D_2} \cdot \Delta D \quad (8a)$$

$$\left|\frac{\Delta R_{D2}}{R_x}\right| = \left|\frac{\partial R_x}{\partial D_2} \cdot \frac{\Delta D}{R_x}\right| = \frac{(2D_3 - D_1 - D_4)}{(D_1 - D_2) \cdot (2D_3 - D_2 - D_4)} \cdot \Delta D \quad (8b)$$

$$\left|\frac{\Delta R_{D3}}{R_x}\right| = \left|\frac{\partial R_x}{\partial D_3} \cdot \frac{\Delta D}{R_x}\right| = \frac{1}{2(D_3 - D_4) - (D_2 - D_4)} \cdot \Delta D \quad (8c)$$

$$\left|\frac{\Delta R_{D4}}{R_x}\right| = \left|\frac{\partial R_x}{\partial D_4} \cdot \frac{\Delta D}{R_x}\right| = \frac{1}{2(D_3 - D_4) - (D_2 - D_4)} \cdot \Delta D \quad (8d)$$

where ΔR_{D1}, ΔR_{D2}, ΔR_{D3}, and ΔR_{D4} represent the individual uncertainties caused by small variations ΔD in the ADC conversion process Therefore, the overall relative uncertainty is given by:

$$\left|\frac{\Delta R_x}{R_x}\right| = \sqrt{\left(\frac{\Delta R_{D1}}{R_x}\right)^2 + \left(\frac{\Delta R_{D2}}{R_x}\right)^2 + \left(\frac{\Delta R_{D3}}{R_x}\right)^2 + \left(\frac{\Delta R_{D4}}{R_x}\right)^2} \quad (9)$$

Notably, errors from R_{ref} can be eliminated by measuring and storing its value within the program. The graphs in Figure 2 illustrate $|\Delta R_x / R_x|$ for a 10-bit ADC across a resistance range of 0.5 to 3.5 kΩ, simulated for an RTD Pt1000 in a three-wire configuration. For the ATmega2560 microcontroller, the typical INL and DNL values are 1.0 and 0.25 LSB, respectively, resulting in a total error of approximately 1.03 LSB, as specified on page 382 of [18]. To determine the optimal R_{ref} that minimizes measurement error, different R_{ref} values were evaluated. Small variations in R_x at lower resistances lead to higher relative uncertainty, whereas at higher resistances, their impact is less significant. Based on these findings, $R_{\text{ref}} = 1$ kΩ was chosen as the optimal value, balancing error across the entire resistance range. Although $R_{\text{ref}} = 0.5$ kΩ reduces error at low R_x, it results in significantly higher errors at larger R_x. In practical implementations, experimental results confirm that actual total errors remain consistently lower than the maximum uncertainty predicted by the simulations in Figure 2, further validating the effectiveness of the proposed setup.

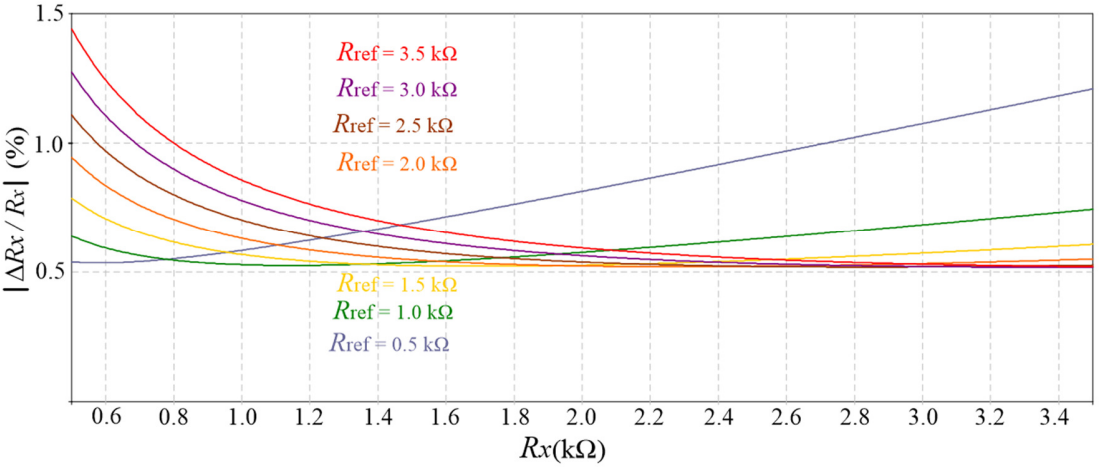

Fig. 2. Measurement uncertainty analysis for varying R_{ref}.

III. EXPERIMENTAL RESULTS

The objective of this experiment is to evaluate the measurement accuracy and uncertainty of three-wire configurations for resistive sensor measurements, specifically targeting an RTD Pt1000.

To simulate practical lead resistance, wire resistances of $R_{\text{w}} = 4.79\ \Omega$ and $R_{\text{w}} = 9.92$, with $R_{\text{w1}} \approx R_{\text{w3}}$, corresponding to cable lengths of approximately 15 and 30 m of 30 AWG (American Wire Gauge) Type C copper, were used [19]. This represents typical conditions encountered in real-world applications. The experimental setup includes an Arduino ATmega2560 board with a supply voltage of $V_{DD} = 4.99$ V, a reference resistor $R_{\text{ref}} = 995.62\ \Omega$, and a sensor resistance R_x varying from 500 to 3,520 Ω. According to the IEC 60751 standard [20], this resistance range corresponds approximately to a temperature range of –100 °C to +850 °C for a Pt1000 sensor, thus encompassing and extending beyond its typical operating limits. Testing over this extended resistance range not only covers the standard range of a Pt1000 but also evaluates the system's accuracy and robustness under extreme conditions, providing valuable insights for calibration and performance optimization. All resistances, including R_{ref} and R_x, were measured using a Keysight 34410A Multimeter to ensure accuracy. Voltage readings were digitized by the Arduino's ADC, with each data point based on an average of 100 samples.

A. Uncertainty Measurement

Figure 3 presents the experimental results of the uncertainty measurement for the proposed method under three different lead-wire resistance conditions: $R_{\text{w}} = 0\ \Omega$, $R_{\text{w}} = 4.79\ \Omega$, and $R_{\text{w}} = 9.92\ \Omega$. The measured resistance values closely align with the actual resistance R_x, confirming the accuracy of the method. The best-fit line represents the ideal relationship between the actual R_x and the measured resistances. For $R_{\text{w}} = 0\ \Omega$, the maximum relative uncertainty is 0.12%, whereas the maximum Nonlinearity Error (NLE) is 0.09%. When $R_{\text{w}} = 4.79\ \Omega$, the maximum relative uncertainty increases slightly to 0.16%, with a maximum NLE of 0.1%. For $R_{\text{w}} = 9.92\ \Omega$, the maximum relative uncertainty is 0.125%, with a maximum NLE of 0.09%. These results demonstrate that the proposed configuration achieves high measurement accuracy with minimal error, even in cases with significant lead-wire resistance, proving its robustness and practicality for resistive sensor measurements in applications requiring long lead wires.

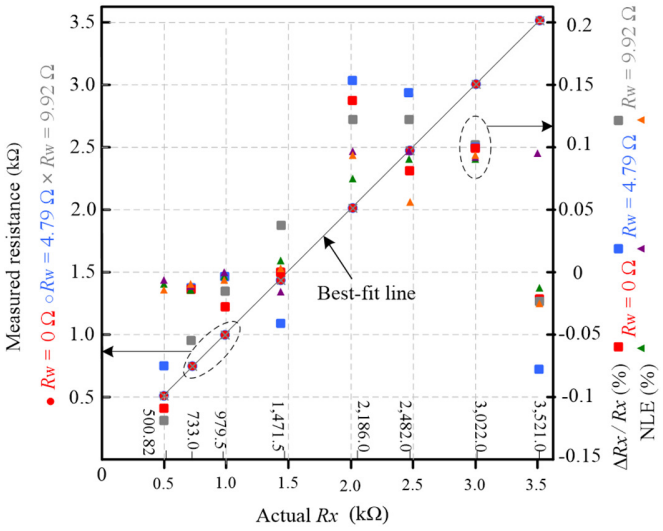

Fig. 3. Measured resistance vs. actual resistance with lead-wire compensation for three conditions: $R_{\text{w}} = 0\ \Omega$, $R_{\text{w}} = 4.79\ \Omega$, and $R_{\text{w}} = 9.92\ \Omega$. The actual resistance R_x values shown in boxes along the x-axis represent the pre-measured test resistors used in the experiments, ranging from 500.82 Ω to 3.52 kΩ.

B. Effect of Variation Wire Resistance

To evaluate the robustness of the proposed method under practical wiring conditions, experiments were conducted using different cable lengths of 5, 10, and 15 m, corresponding to increasing values of lead-wire resistance R_{w}. The results show that the proposed configuration maintains a relative error within 0.16% across all tested lengths when $R_{\text{w1}} \approx R_{\text{w3}}$, confirming its effectiveness in compensating for symmetrical lead resistance. Figure 4 illustrates the measured resistance for

a fixed sensor value of $R_x = 2{,}186\ \Omega$, tested across the three cable lengths. The measurements demonstrate minimal deviation (less than 0.16%), confirming that lead resistance has a negligible effect when symmetry is maintained.

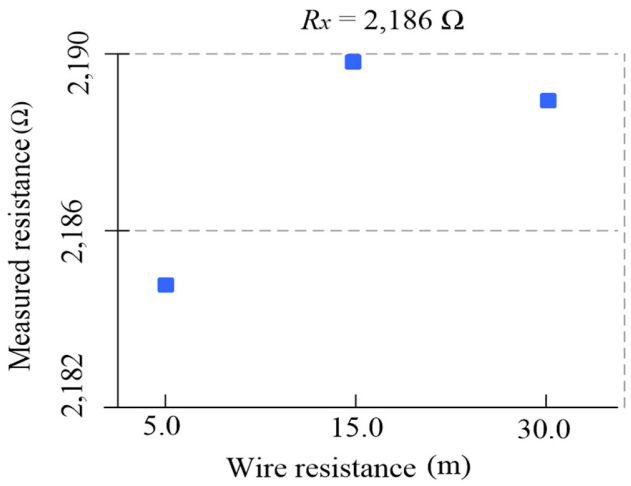

Fig. 4. Effect of varying lead-wire resistance on measured resistance. The reference sensor resistance $R_x = 2{,}186\ \Omega$ was measured using 5, 15, and 30 m cable lengths (corresponding to $R_w = 1.6\ \Omega$, $R_w = 4.79\ \Omega$, and $R_w = 9.92\ \Omega$).

However, when the lead-wire resistances are mismatched—specifically when $R_{w1} \neq R_{w3}$ —the measurement error increases due to the term $R_{w1} - R_{w3}$ in (4). This mismatch introduces an offset in the measured voltage drop across the sensor, leading to deviation from the ideal linear response. Although this effect was not extensively quantified in this study, (4) clearly indicates that the error is directly proportional to the difference$R_{w1} - R_{w3}$. Such conditions may arise from asymmetric wiring or unequal cable routing and highlight the importance of maintaining balanced lead resistances for optimal accuracy in practical implementations.

IV. DISCUSSION AND COMPARISON

The proposed circuit offers a significantly simpler hardware implementation compared to existing techniques. As summarized in Table I, many prior works rely on complex AFE designs that incorporate multiple operational amplifiers, analog switches, constant voltage or current sources, and numerous passive components such as resistors and capacitors [6, 8, 10, 11]. These circuits, while capable of achieving accurate results, typically require careful calibration, increased board space, higher power consumption, and result in greater overall cost and complexity. In contrast, the proposed method uses only a single precision reference resistor in conjunction with the ADC channels and digital output pins of a standard microcontroller. It does not require additional active components such as op-amps or voltage regulators, making it easy to implement in embedded systems. This direct interface approach reduces the external component count, resulting in a compact, cost-effective, and energy-efficient solution while still delivering high measurement accuracy.

While the proposed method shows slightly higher measurement errors compared to some R-to-V techniques [10, 11], it is important to note that those techniques produce an analog voltage output that must be further digitized by an ADC. This additional conversion stage can introduce quantization errors, offset drift, and gain inaccuracies, especially in noisy or power-constrained environments. On the other hand, the proposed method directly utilizes the ADC for resistance calculation, eliminating such intermediate conversion sources of error. The DIC approach in [12] achieves very low maximum relative error, but this performance is under ideal test conditions. In practical scenarios, variations in supply voltage and interference can degrade its performance, as discussed in [14]. Meanwhile, our prior work [17] achieved similarly low error levels by employing two stabilizing resistors and a tuning technique to balance supply variation and ADC inaccuracy. However, this came at the expense of increased circuit complexity and calibration effort.

TABLE I. SUMMARY OF COMPARISON STUDY WITH EXISTING TECHNIQUES

Ref., year	AFE	DIC	Conversation type	Range (Ω)	Max. NLE (%)	Max. relative error (%)
[6], 2022	4 switches, 1 op-amp, 5 resistors, 1 capacitor (DIR-1 configuration)	-	R-to-T	[80, 150], [800, 1500]	0.09	0.29, 0.22
[8], 2024	3 op-amps, 2 switches, 2 resistors, 1 capacitor	-	R-to-T	[60, 390]	0.15	0.50
[10], 2023	2 op-amps, 1 resistor, 2 matched resistors (IC3 R configuration)	-	R-to-V	[80, 200], [800, 2000]	0.20, 0.05	0.62, 0.32
[11], 2024	(1) 2 diodes, 1 op-amp (2) 2 switches, 1 op-amp, 1 resistor, low pass filter circuit	-	R-to-V	[63, 267]	0.005	-
[12], 2022	-	3 resistors and 1capacitor	R-to-T (5 I/O pins)	[60, 264]	0.03	0.02
[17], 2025	-	Two stabilizing resistors and a precision reference resistor	R-to-V (4 channels, 1 ADC)	[50, 317]	-	0.09
This work	-	A precision reference resistor	R-to-V (4 channels, 1 ADCs, 2 I/O pins)	[500, 3500]	0.10	0.16

Note: Relative error (%) follows reported values from each work. This study uses $|\Delta R_x/R_x|$ or total relative uncertainty.

In summary, the proposed configuration offers a favorable trade-off between accuracy, simplicity, and implementation cost. It is particularly well-suited for embedded applications where hardware simplicity, low power consumption, and acceptable measurement accuracy are essential. While the absence of stabilizing resistors can lead to increased excitation current—especially when measuring low resistance values—the total power consumption of the measurement circuit (excluding the microcontroller) remains modest, estimated at approximately 5–15 mW, depending on the sensor resistance. This supports its suitability for low-power applications.

In practice, this level of power consumption is acceptable for many real-world scenarios, particularly those involving high-resistance sensors (e.g., RTDs above 1 kΩ or resistive elements in the 1–3.5 kΩ range), where the resulting current remains within safe and energy-efficient limits. Thus, despite the slightly higher current path, the proposed method remains a practical and efficient solution for a wide range of resistive sensing applications.

V. CONCLUSIONS

This paper proposed a simple and effective three-wire configuration for resistive sensor measurement using the Analog-to-Digital Converters (ADCs) of microcontrollers. The approach compensates for lead-wire resistance and mitigates supply voltage and internal resistance effects through ratiometric voltage measurements, without the need for complex Analog Front-End (AFE) circuitry. By leveraging the internal features of microcontroller pins and minimizing external components, the design enables compact and efficient implementation.

Experimental validation demonstrated a maximum relative error of only 0.16% across a wide resistance range of 500–3,500 Ω, confirming the method's accuracy, stability, and robustness under various lead-wire conditions. Compared to existing methods, the proposed configuration offers a favorable balance between hardware simplicity, cost-efficiency, and measurement performance. This makes it particularly suitable for embedded systems and low-power applications, including Internet of Things (IoT) devices, remote monitoring platforms, and portable instrumentation.

Future work may focus on extending the proposed approach to support higher resistance ranges and four-wire configurations for applications with stricter accuracy requirements. Enhancing ADC resolution could further improve precision, whereas exploring dynamic compensation or calibration-free techniques may increase robustness and ease of deployment in field conditions.

ACKNOWLEDGMENT

This research project was financially supported by Mahasakham University, Thailand.

REFERENCES

[1] R. Pallás-Areny and J. G. Webster, *Sensors and Signal Conditioning*, 2nd ed. Hoboken, NJ, USA: John Wiley & Sons, 2012.

[2] "Understanding RTDs." TE connectivity, 2016, [Online]. Available: https://www.te.com/content/dam/te-com/documents/sensors/global/te-sensor-solutions-applicationnote-understanding-RTDs.pdf.

[3] Keithley Instruments, "Overview of two-wire and four-wire (Kelvin) resistance measurements, " Application Note 3176, Cleveland, OH, USA, May 2012. [Online]. Available: http://www.tek.com/sites/tek.com/files/media/document/resources/2110_2Wire4WireKelvinResistanceAppNote.pdf.

[4] P. R. Nagarajan, B. George, and V. J. Kumar, "Improved Single-Element Resistive Sensor-to-Microcontroller Interface," *IEEE Transactions on Instrumentation and Measurement*, vol. 66, no. 10, pp. 2736–2744, Oct. 2017, https://doi.org/10.1109/TIM.2017.2712918.

[5] F. Reverter, A. Chandrika Sreekantan, and B. George, "Circuits for the Measurement of Remote Resistive Sensors: A Review," *IEEE Transactions on Instrumentation and Measurement*, vol. 74, pp. 1–13, 2025, https://doi.org/10.1109/TIM.2025.3542136.

[6] K. Elangovan, A. Antony, and A. Chandrika Sreekantan, "Simplified Digitizing Interface-Architectures for Three-Wire Connected Resistive Sensors: Design and Comprehensive Evaluation," *IEEE Transactions on Instrumentation and Measurement*, vol. 71, pp. 1–9, 2022, https://doi.org/10.1109/TIM.2021.3136176.

[7] E. K and A. Chandrika Sreekantan, "An Efficient Digital Readout for Four-Lead Resistance Thermometers," *IEEE Sensors Letters*, vol. 7, no. 12, pp. 1–4, Dec. 2023, https://doi.org/10.1109/LSENS.2023.3330115.

[8] K. Elangovan, "A Novel Triple-Slope-Based Digital Measurement Platform for Three-Wire Connected Resistive Sensors," *IEEE Transactions on Instrumentation and Measurement*, vol. 73, pp. 1–3, 2024, https://doi.org/10.1109/TIM.2024.3411132.

[9] S. K. Sen, T. K. Pan, and P. Ghosal, "An improved lead wire compensation technique for conventional four wire resistance temperature detectors (RTDs)," *Measurement*, vol. 44, no. 5, pp. 842–846, Jun. 2011, https://doi.org/10.1016/j.measurement.2011.01.019.

[10] T. Mathew, K. Elangovan, and A. C. Sreekantan, "Accurate Interface Schemes for Resistance Thermometers With Lead Resistance Compensation," *IEEE Transactions on Instrumentation and Measurement*, vol. 72, pp. 1–4, 2023, https://doi.org/10.1109/TIM.2023.3291739.

[11] F. Reverter, "Two Proposals of a Simple Analog Conditioning Circuit for Remote Resistive Sensors with a Three-Wire Connection," *Sensors*, vol. 24, no. 2, Jan. 2024, Art. no. 422, https://doi.org/10.3390/s24020422.

[12] F. Reverter, "A Microcontroller-Based Interface Circuit for Three-Wire Connected Resistive Sensors," *IEEE Transactions on Instrumentation and Measurement*, vol. 71, pp. 1–4, 2022, https://doi.org/10.1109/TIM.2022.3219492.

[13] F. Reverter, "A direct approach for interfacing four-wire resistive sensors to microcontrollers," *Measurement Science and Technology*, vol. 34, no. 3, Dec. 2022, Art. no. 037001, https://doi.org/10.1088/1361-6501/aca425.

[14] F. Reverter, M. Gasulla, and R. Pallas-Areny, "Analysis of Power-Supply Interference Effects on Direct Sensor-to-Microcontroller Interfaces," *IEEE Transactions on Instrumentation and Measurement*, vol. 56, no. 1, pp. 171–177, Feb. 2007, https://doi.org/10.1109/TIM.2006.887401.

[15] Z. Czaja, "Simple Measurement Method for Resistive Sensors Based on ADCs of Microcontrollers," *IEEE Sensors Journal*, vol. 24, no. 3, pp. 2996–3003, Feb. 2024, https://doi.org/10.1109/JSEN.2023.3341214.

[16] S. M. A. Ghaly, "LabVIEW Based Implementation of Resistive Temperature Detector Linearization Techniques," *Engineering, Technology & Applied Science Research*, vol. 9, no. 4, pp. 4530–4533, Aug. 2019, https://doi.org/10.48084/etasr.2894.

[17] W. Khamsen, A. Aurasopon, and C. Takeang, "Simplified Three-Wire and Four-Wire Interface for Resistive Sensor Measurement Using Microcontroller ADCs," *IEEE Transactions on Instrumentation and Measurement*, vol. 74, pp. 1–10, 2025, https://doi.org/10.1109/TIM.2025.3578689.

[18] "ATmega640/V-1280/V-1281/V-2560/V-2561/V, 8-bit Microcontroller with 16/32/64KB In-System Programmable Flash (Datasheet)."

Microchip, [Online]. Available: https://ww1.microchip.com/downloads/en/devicedoc/atmega640-1280-1281-2560-2561-datasheet-ds40002211a.pdf.

[19] "Wire Gauge Table." Calmont Wire & Cable, [Online]. Available: https://www.calmont.com/wp-content/uploads/calmont-eng-wire-gauge.pdf.

[20] "Industrial platinum resistance thermometers and platinum temperature sensors." Geneva, Switzerland, Jan. 2022, 2025. [Online]. Available: https://cdn.standards.iteh.ai/samples/102478/eb22a33147f842f7a71ab9db245d92ba/IEC-60751-2022.pdf.